

Oculomotor inhibition during smooth pursuit and its dependence on contrast sensitivity

Inbal Ziv

School of Optometry and Vision Science, Faculty of Life Science, Bar-Ilan University, Ramat Gan, Israel



Yoram S. Bonneh

School of Optometry and Vision Science, Faculty of Life Science, Bar-Ilan University, Ramat Gan, Israel



Our eyes are never still, but tend to "freeze" in response to stimulus onset. This effect is termed "oculomotor inhibition" (OMI); its magnitude and time course depend on the stimulus parameters, attention, and expectation. We previously showed that the time course and duration of microsaccade and spontaneous eye-blink inhibition provide an involuntary measure of low-level visual properties such as contrast sensitivity during fixation. We investigated whether this stimulus-dependent inhibition also occurs during smooth pursuit, for both the catch-up saccades and the pursuit itself. Observers followed a target with continuous back-and-forth horizontal motion while a Gabor patch was briefly flashed centrally with varied spatial frequency and contrast. Catch-up saccades of the size of microsaccades had a similar pattern of inhibition as microsaccades during fixation, with stronger inhibition onset and faster inhibition release for more salient stimuli. Moreover, a similar stimulus dependency of inhibition was shown for pursuit latencies and peak velocity. Additionally, microsaccade latencies at inhibition release, peak pursuit velocities, and latencies at minimum pursuit velocity were correlated with contrast sensitivity. We demonstrated the generality of OMI to smooth pursuit for both microsaccades and the pursuit itself and its close relation to the low-level processes that define saliency, such as contrast sensitivity.

an increase of eye movements, resulting from stimulus onset (Bonneh et al., 2015; Engbert & Kliegl, 2003; Rolfs, 2009; Rolfs et al., 2008). A series of articles were published on OMI and its affinity to contrast sensitivity, all of which were conducted during fixation, for both microsaccades and spontaneous eye blinks (Bonneh et al., 2015; Bonneh et al., 2016; Denniss, Scholes, McGraw, Nam, & Roach, 2018; Engbert & Kliegl, 2003; Scholes, McGraw, Nyström, & Roach, 2015). Our initial motivation for conducting the current study was to investigate whether the OMI generalizes to smooth pursuit in terms of inhibiting the catch-up saccades, as well as suppressing the pursuit movement itself, similar to the OMI effect at fixation, which we have previously investigated (Bonneh et al., 2015; Bonneh et al., 2016). If so, then this supports the notion of a common and general OMI mechanism. We presented the initial results of the current study at two conferences, focusing on OMI driven by the low-level properties of the stimulus (Ziv & Bonneh, 2017; Ziv & Bonneh, 2019). More recent studies have found evidence of catch-up saccade inhibition during pursuit that is similar to microsaccade inhibition during fixation (Badler, Watamaniuk, & Heinen, 2019; Buonocore, Skinner, & Hafed, 2019; see also an earlier work of Kerzel, Born, & Souto, 2010). These studies established the background for our study, which focuses on the effect of the low-level features of the stimuli on a common OMI mechanism and on its relationship to contrast sensitivity thresholds.

Microsaccades, which are considered to be a part of “fixational eye movements” (see a review in Martinez-Conde, Macknik, & Hubel 2004), are small, fast, and involuntary eye movements. Microsaccades have been implicated in many studies of perception, attention, and cognition (Engbert 2006; Pastukhov & Braun 2010; Laubrock et al. 2010; see a review in Rolfs 2009). In addition, they were found to be inhibited in response to perceptual events for a duration that depends on the stimulus parameters, anticipation, and attention (Bonneh et al., 2013; Bonneh et al., 2010;

Introduction

Our eyes are constantly moving, even when maintaining still fixation (Barlow, 1952). Eye movements during fixation, termed fixational eye movements, are often inhibited after a transient stimulus onset, a phenomenon known as oculomotor inhibition (OMI) (Bonneh, Adini, & Polat, 2015; Bonneh, Adini, & Polat, 2016; Rolfs, Kliegl, & Engbert, 2008; Valsecchi, Betta, & Turatto, 2007; White & Rolfs, 2016). OMI can also be described as a “freeze effect”; it has a stereotypical pattern of decrease, followed by

Citation: Ziv, I., & Bonneh, Y. S. (2021). Oculomotor inhibition during smooth pursuit and its dependence on contrast sensitivity. *Journal of Vision*, 21(2):12, 1–20, <https://doi.org/10.1167/jov.21.2.12>.



Rolfs et al., 2008). Furthermore, recent studies have shown a correlation between microsaccade inhibition and contrast sensitivity (Bonneh et al., 2015; Scholes et al., 2015); Denniss et al. (2018) demonstrated a method for estimating contrast sensitivity from the microsaccade rate modulation in response to transient stimuli (Denniss et al., 2018).

Smooth pursuit is a type of eye movement that enables the visibility of a moving target. It is accompanied by corrective saccades known as “catch-up saccades” to avoid position and velocity errors (de Brouwer, Missal, Barnes, & Lefèvre, 2002; de Brouwer, Yuksel, Blohm, Missal, & Lefèvre, 2002). Other factors can trigger catch-up saccades, such as the predicted position error (Nachmani, Coutinho, Khan, Lefèvre, & Blohm, 2020) and pursuing a foveal target (Heinen, Badler, & Watamaniuk, 2018; Heinen, Potapchuk, & Watamaniuk, 2016). Importantly, recent studies have found pursuit inhibition and catch-up saccade inhibition in response to briefly flashed stimuli (Buonocore et al., 2019; Kerzel et al., 2010). Kerzel et al. (2010) presented flashed Gabor stripes with a fixed eccentricity and varied contrast while observers were engaged in pursuit. They found that the inhibition, for both the catch-up saccades and the pursuit itself, was shorter in latency and longer in duration (i.e., it took a longer time before it was released) for a higher contrast. However, they did not investigate the relation of this effect to contrast sensitivity. Previous psychophysical experiments showed similar contrast sensitivity during fixation and smooth pursuit (Flipse, Wildt, Rodenburg, Keemink, & Knol, 1988; Murphy, 1978); however, other studies showed attenuated contrast sensitivity during pursuit when a target was flashed at the periphery (Schütz, Braun, & Gegenfurtner, 2007; Schütz, Delipetkos, Braun, Kerzel, & Gegenfurtner, 2007). This suggests that oculomotor measures for contrast sensitivity could also be obtained during smooth pursuit when the contrast patch is placed in the center of the pursued target.

In the current study, we investigated the effect of OMI during smooth pursuit and its relation to contrast sensitivity. We were partly driven by the need to assess contrast sensitivity in populations that find prolonged fixation difficult, such as infants, and partly by the desire to better understand the essence and function of the OMI phenomenon. To test OMI during smooth pursuit, we briefly flashed a vertical Gabor patch while observers were pursuing a circular target in two main experiments: varied spatial frequency (fixed contrast) and varied contrast (fixed spatial frequency). In line with the general OMI hypothesis, we expected to find a catch-up saccade inhibition that is shorter for higher contrast and longer for higher spatial frequency (above 2cpd), as previously found at fixation (Bonneh et al., 2015; Bonneh et al., 2016). We also expected to find a slowdown of the pursuit itself that is stronger

for higher contrast and weaker for higher spatial frequencies. Furthermore, we expected to find that contrast sensitivity (detection thresholds) for different spatial frequencies and the OMI that we measured (catch-up saccade, as well as pursuit speed inhibition) are correlated.

We found that both catch-up saccades and the smooth pursuit itself were inhibited after a flashed superimposed stimulus, and that these inhibition effects depended on the stimulus contrast and the spatial frequency; a faster inhibition onset and a faster release of inhibition occurred for more salient stimuli. Moreover, these inhibition effects were also correlated with the contrast sensitivity of the thresholds, measured psychophysically.

Methods

Participants

Overall, 23 adults (ages 18–42) with normal or corrected-to-normal vision and with no known neurological disorders participated in the study. Vision was estimated before participation by an authorized optometrist. Twenty subjects were tested on the spatial frequency tasks, and 18 subjects were tested on the contrast task. Three additional experiments were conducted for a control: the contrast sensitivity task (12 subjects), the fixation task (15 subjects), and smooth pursuit without distractors (10 subjects). Fifteen subjects participated in both the spatial frequency and contrast experiments; seven of them participated in all the experiments (see Experiments 1–5 in the Methods). This study was approved by the Institutional Review Board ethics committee of Bar-Ilan University.

Apparatus

Stimuli were displayed on an Eizo FG2421 24" HD monitor with a 1920×1080 pixel resolution and a 100 Hz refresh rate. The monitor was designed for gaming and was found suitable for visual psychophysics because of its high temporal accuracy (Ghodrati, Morris, & Price, 2015). The stimuli were presented using an in-house-developed platform for the psychophysical and eye-tracking experiments (PSY) developed by Yoram S. Bonneh, running on a Windows PC. Eye movements were recorded using the EyeLink 1000 infrared system (SR Research, Ontario, Canada), with a sampling rate of 500 Hz, a 35 mm lens, and a head and chin rest. Under these conditions, the EyeLink system is known to have a spatial resolution of 0.01° and an average accuracy of 0.25° to 0.5° . All recordings were done binocularly; analyses were done on data from the

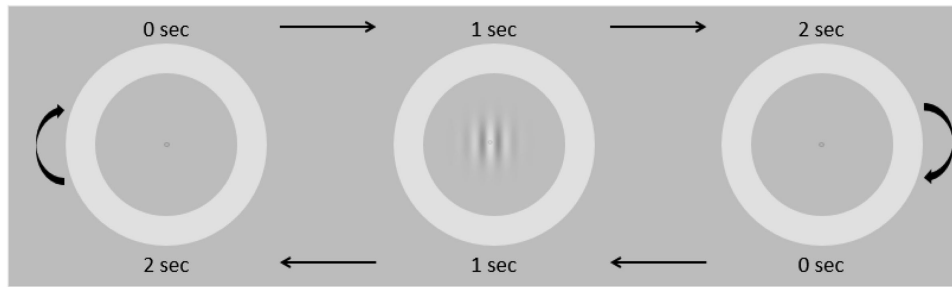


Figure 1. The experimental paradigm for contrast and spatial frequency detection during pursuit. A circular ring (with an external size of $\sim 7.7^\circ$ and an internal size of $\sim 6.2^\circ$) surrounded a small fixation circle (size $\sim 0.1^\circ$), moved smoothly at $6.2^\circ/\text{sec}$ from right to left and vice versa. The subjects were asked to track the fixation circle. Each direction represents one trial, two seconds long. When the stimulus reached the center, a Gabor patch was flashed for 100 ms at the middle of the moving target in a pseudo-random order. The spatial frequency and the contrast of the Gabor patch were manipulated in two different experiments (see the Methods).

		Spatial Frequency (cyc/°)						Contrast (%)										
		1	2	3	4	6	8	No Gabor	50	25	12.5	6.25	3.13					
Smooth Pursuit	msRT-On	Experiment 1						Experiment 3						Experiment 2				
	msRT-Off																	
	Min-vel-lat																	
	Max-vel-lat																	
	Max-vel																	
Fixation	Threshold	Experiment 4																
	msRT-On	Experiment 5						Bonneh et al. (2015)										
	msRT-Off																	

Table 1. Summary of the experimental paradigms. The independent conditions were presented at the top of the table, and the dependent measurement types were presented on the left of the table. The results of the contrast during fixation were taken from [Bonneh et al. \(2015\)](#) and presented for comparison between msRT during fixation and smooth pursuit.

msRT-on-inhibition onset, latency of the last microsaccade in an early time window (0-200 ms); msRT-off-inhibition offset, latency of the first saccade at the inhibition release time window (200-800 ms); Min/Max-vel-lat, min/max velocity peak latency (100-400 ms and 300-700ms, respectively); Max-vel-velocity maximum peak (300-700 ms).

left eye. A standard nine-point calibration was used before each session. The sitting distance was 0.6 m; the background luminance was $\sim 32 \text{ cd/m}^2$ after gamma correction; all experiments were conducted in dim light.

Stimuli and procedure

In three eye-tracking experiments (spatial frequency, contrast, and pursuit without distractors), subjects were asked to follow a small circle (0.1°) with a luminance of $\sim 23 \text{ cd/m}^2$; it was surrounded by a ring with an external size of 7.7° (radius of 3.85°), an internal size of 6.2° (radius of 3.1°), and with a luminance of $\sim 35 \text{ cd/m}^2$ ([Figure 1](#)). The whole stimulus constantly moved horizontally back and forth at $6.2^\circ/\text{sec}$, two seconds per direction, creating a periodic stimulus with a triangular waveform, manifested by the eyes' horizontal position, shown in [Figures 4a](#) and [5a](#). While

the observer followed the target, a vertical Gabor patch with a fixed envelope of $\sigma = 1.24^\circ$ was flashed, midway at the center of the moving target, for 100 ms at 0.5 Hz (i.e., every two seconds, see [Figure 1](#)). In each experiment, the Gabor patches with varied contrast or spatial frequency were presented in a pseudo-random order for each condition, via a pre-computed random permutation that ensured an accurate number of trials. There were 20 trials per condition and 10 trials per direction (left/right) in each run. Each observer was tested on several runs, 100 trials in total for each condition (see more details below for each experiment and in the summary table in [Table 1](#)).

Experiment 1: Spatial frequency experiment

The presented spatial frequencies of the Gabor patches were 1, 2, 3, 4, 6, and 8 cyc/° and with a fixed

contrast of 25%, 20 trials for each frequency in random order, 10 trials per direction, 120 trials for a ~4-minute run; five runs in total.

Experiment 2: Contrast experiment

The presented contrasts of the Gabor patches were 3.125%, 6.25%, 12.5%, 25%, and 50%, and with a fixed spatial frequency of 3 cyc/°, 20 trials for each contrast in random order, 10 trials per direction, 100 trials for a ~3.5-minute run; five runs in total.

Experiment 3: Smooth pursuit without a flashed Gabor

No distractors (Gabor patches) were presented; all the rest was identical to the previous experiment. The subjects were tested for one run with 100 trials in total, 50 per direction. This condition was necessary for determining the onset and duration of the steady-state smooth pursuit without distractors.

Experiment 4: Contrast sensitivity function

Twelve subjects were tested on the psychophysical contrast detection threshold as a function of spatial frequency. The same method was previously applied by [Bonneh et al. \(2015\)](#) for measuring the contrast detection threshold as a function of spatial frequency; the details are summarized here and in [Bonneh et al. \(2015\)](#). The detection thresholds were measured using a standard 3:1 temporal two-alternative forced-choice staircase procedure with a 0.1 log-unit step, for each spatial frequency used in experiment 1. Each trial was initiated with a button press while fixating on a small fixation circle (0.26° diameter). The fixation circle was erased after 200 ms, followed by a blank interval of 500 ms, followed by two 100 ms stimulus displays with 500 ms between them. The two displays were denoted by four white crosses (2.6° width and height) with an eccentricity of 7.7°. A vertical Gabor patch with an envelope of $\sigma = 2^\circ$ was presented in one of the two displays, while the subject reported target identification by pressing the mouse button to report the display of the target (first or second). Auditory feedback was given for errors. All frequency conditions were randomly interleaved with independent staircases. A staircase was terminated after eight reversals; the first two reversals were removed from the average. The threshold was determined as the geometric mean of the last six reversals. Each participant was tested for three runs.

Experiment 5: The fixation task

This experiment was identical to experiment 1, except that there was no target motion and the subjects were asked to maintain fixation on a static small circle (0.1°) surrounded by a static bright ring. A Gabor patch with a fixed contrast of 25% and spatial frequencies of 1, 2, 3, 4, 6, and 8 cyc/° (as in experiment 1) was flashed for 100 ms at 0.5 Hz. All conditions were presented in random order and with an additional no-Gabor condition, 20 trials per condition, 140 trials per run. Each observer was tested on five runs lasting for ~4.7 minutes each.

Data analysis

The data analysis was similar to that applied in our previous studies ([Bonneh et al., 2015](#); [Bonneh et al., 2016](#); [Bonneh et al., 2010](#); [Yablonski, Polat, Bonneh, & Ben-Shachar, 2017](#)), with additional analyses developed for pursuit velocity, all detailed below.

Microsaccade detection

Microsaccades were detected using the algorithm introduced by [Engbert and Kliegl \(2003\)](#) and were similar to the ones used by [Bonneh et al. \(2015\)](#) and [Yablonski et al. \(2017\)](#), along with small parameter changes. Data were initially smoothed using a local linear regression fitting (LOWESS method), with a window of 25 ms to optimize microsaccade extraction. Microsaccades were detected when the horizontal and vertical velocities exceeded a threshold of eight median standard deviations ($\lambda = 8$) of the velocities. The permitted velocity range was 8°/sec to 150°/sec, with an amplitude range of 0.08° to 2° and a minimum duration of 9 ms. A linear relation between microsaccade peak velocity and magnitude, known as the “main sequence” ([Bahill, Clark, & Stark, 1975](#)), was verified.

Blink detection

Blinks were detected as in [Yablonski et al. \(2017\)](#). Their detection served only for the purpose of removing their trace in calculating pursuit velocity. Blinks were defined as periods of data with zero pupil size. Then, the vertical trace was analyzed to detect the blink onset and offset; they were defined as the time when the change in the vertical trace passed a threshold of 4 *SD* from the average of the first 1/3 part of the selected window, which was set to 100 ms before and 150 ms after each blink. Blinks outside the range of 250 to

700 ms were rejected as possibly reflecting measurement noise.

Epoch extraction

Epochs were extracted and time-locked to the stimulus onset (Gabor onset was set to time zero), with one epoch per stimulus presentation, which represented one trial.

Microsaccade rate modulation

The microsaccade rate modulation was calculated by first convolving a raw rate estimate of one microsaccade per sample duration (2 ms) at the time of onset with a Gaussian kernel ($\sigma = 50\text{ms}$) (see [Bonneh et al., 2010](#) and [Bonneh, Adini, & Polat, 2015](#)). After the data were segmented into epochs time-locked to the Gabor onset (set to time zero), the rates were first averaged and normalized across epochs within participants, then across participants and readjusted by the grand average, to compute the event-related modulation of microsaccades with equal contribution from each participant. The error bars were calculated as 1 *SE* of the mean across observers.

Microsaccade reaction time (msRT)

A measure of the microsaccade “response time” was calculated for each epoch relative to the stimulus onset as the latency of the last microsaccade in the window of the inhibition onset (early) and the latency of the first microsaccade in the window of the release (late), as was done in a previous study ([Bonneh et al., 2015](#)). Epochs without microsaccades within the selected windows were excluded from the average. To assess the statistical significance of the msRT modulation effects, we used the Linear Mixed Model (LMM) on averaged data. We also applied normalization for proper error bars and the presentation of scatter plots (see the “Data Normalization” part below). The rationale for using msRT rather than analyzing the rate modulation functions is based on the idea that discrete data could be analyzed better in their discrete form rather than first computing continuous rate modulation estimates and then computing measures on these estimates. We preferred to use the discrete measures when they exist (unlike the pursuit speed, which is originally continuous). The disadvantage of the msRT measure lies in its dependence on the temporal ROI and on the existence of microsaccades in the ROI, where trials without microsaccades are ignored without affecting the msRT. This may create a discrepancy between msRT and the rate modulation functions.

Extraction of pursuit velocity

Pursuit velocities were calculated from the raw data of the horizontal traces. First, blinks and saccades were removed from the raw traces with 100 ms margins for blinks and 30 ms margins for saccades; then the horizontal trace was normalized by subtracting the mean of each run and all data above 2 standard deviations were ignored in order to limit the data obtained from changes in the pursuit direction and the beginning and the end of each recorded run, leaving the main effect in each trial where the stimulus was flashed. In addition, the deleted areas did not take place in an additional analysis of the OMI measures such as the minimum and maximum velocity peaks. Then, we used a series of filters as in [Goettker et al. \(2018\)](#) to smooth the data and to extract pursuit velocity, as follows: all missing data from the horizontal trace were interpolated with a linear interpolation, to allow for signal filtering. Next, the data were filtered with a second-order Butterworth filter with a cutoff frequency of 30Hz and the eye velocity was calculated using derivatives from the horizontal trace; it represents the local speed between successive samples. This calculation of the local speed gave the same results as a calculation made on data after removing microsaccades and aligning the gaps. Then, the eye velocity was filtered with another second-order Butterworth filter with a cutoff frequency of 20Hz. Finally, all the interpolated data associated with the detected saccades and blinks were marked to be ignored and were not taken into account in the calculations that followed.

Pursuit peak velocity and peak latency

Velocity peaks and latencies were calculated in separate windows due to the nature of the experiment and the pursuit time course. Pursuit minimum and maximum velocities and latencies were calculated per epoch as the time from the stimulus onset to the minimum/maximum velocity peak, with peak values averaged in a window of ± 20 ms around the actual peak to reduce noise. The data were normalized for proper error bars and to present the scatter plots (see the “Data Normalization” part below). Note that when comparing the peaks of the average velocity traces to the estimated peaks computed per observer and averaged across observers, they may exhibit different latencies and peak velocities due to the variability of the individual traces.

Data normalization

To remove the effect of variability induced by tonic differences in the different parameters across

observers (e.g., overall slow and fast observers) on the data presented, we averaged and normalized the data by subtracting the mean within observers and then added the total mean across observers and conditions to produce individual scatter plots (light blue in the plots), as well as averages across observers (dark blue in the plots), with error bars calculated as 1 SE of the normalized and corrected mean (Cousineau, 2005). All observers' results were taken into account in the average calculation; observers' averages outside the plots were recorded on the border of each plot in gray, low averages were recorded on the bottom of the plot and vice versa. The total number of points outside the plot was recorded in each plot legend.

Assessment of the statistical significance

The statistical tests we used were as follows: the LMM, Pearson's linear correlation, and the nonparametric permutation test. LMM was used to assess the significance in msRT, the pursuit latencies, and the pursuit peak velocity in cases of contrast and spatial frequency using the mean results of each observer per condition and readjustment with the total mean across observers and conditions (i.e., 120 points in spatial frequency and 90 points in contrast). This statistical method was previously used in analyzing eye movements (for example: Kliegl, 2007; Hohenstein, Matuschek, & Kliegl, 2017). The responses were fitted to a simple model of maximum likelihood with one predictor variable set for the flashed Gabor parameters (i.e., spatial frequency or contrast) and the random effect set as the observer's variability. For each case, we computed the standard error (SE), the regression coefficient (b), the t -test (t), and the p value of the LMM (p_{lmm}) at a 95% confidence level. In addition, we computed Pearson's linear correlation coefficient (r^2) for the group averages of each plot; the mean was calculated as the average and normalized data within observers, then averaged across observers and finally readjusted with the total average across all conditions and observers. Sometimes we also used a nonparametric permutation test (Efron & Tibshirani, 1994) to assess the significance. We used 1000 random permutations on the observation labels in each test. The labels represent the stimuli of each epoch in each experiment (i.e., the contrast or spatial frequency). We quantified the effect by using the correlation coefficient R in each graph and computed the p value as the fraction of permutations in which the original correlation was exceeded by the correlation of the permuted data. See the methods of Yablonski et al. (2017) and Bonneh, Adini, and Polat (2016) for our previous use of this method.

Results

The results for the three pursuit experiments for contrast, spatial frequency, and control, including the microsaccade and pursuit inhibition analyses, are summarized below, followed by a comparison of the data with the psychophysical measures of contrast sensitivity and fixation.

Microsaccade inhibition and spatial frequency

The results of the effect of spatial frequency on microsaccade inhibition during pursuit are shown in Figure 2 (see Experiment 1 in the Methods). The rate modulation functions are shown in Figure 2b; they show an earlier and robust inhibition as well as an earlier and stronger release from inhibition for the low spatial frequency (1 cyc/°), compared with the higher spatial frequencies (6–8 cyc/°). The same effect can be noted in the raster plots (Figure 2a) at 1 and 6 cyc/°. The data show an ordered pattern of rate modulation (Figure 2b) from low to high spatial frequency for both the onset of inhibition, around 200 ms, and its release, around 400 ms. The rate modulation functions were used to set the basis for computing the discrete measures of msRT, as shown in Figures 2c and 2d. The msRTs were calculated as a measure for determining the time of inhibition onset in an early time window of 0–200 ms (0 represents the stimulus onset), and the inhibition release in a late time window of 200 to 800 ms after the stimulus onset (see the Methods for more details and Bonneh, Adini, and Polat (2015) for a similar analysis). The msRT in both time windows increased roughly linearly as a function of spatial frequency, from 1 cyc/° up to 8 cyc/°; both the inhibition onset and release latencies were faster at lower spatial frequencies (more salient stimuli), starting as early as ~73 ms for 1 cyc/° in the inhibition onset window and ~445 ms in the inhibition release window. The LMM statistics revealed the following values: $\beta_1 = 4.40$ (2.76, 6.05) with $SE = 0.83$ and $t(118) = 5.29$ in the inhibition onset window and $\beta_1 = 5.69$ (3.93, 7.46), $SE = 0.89$, and $t(118) = 6.38$ in the inhibition release window; the p value of LMM was found to be significant ($p < 0.005$) in both time windows, showing deviation from a straight line (a nonzero linear relationship). The slope in the inhibition release window ($\beta_1 = 5.69$) was higher than that in the inhibition onset window ($\beta_1 = 4.40$), indicating a greater temporal change for changes in spatial frequency. An additional correlation test between msRT and the spatial frequency showed values of $r^2 = 0.69$ for the inhibition onset and $r^2 = 0.92$ for the inhibition release, both significant ($p = 0.039$ and $p = 0.003$, respectively). The nonparametric permutation test showed values of $p_{\text{mc}} = 0.018$ in the inhibition

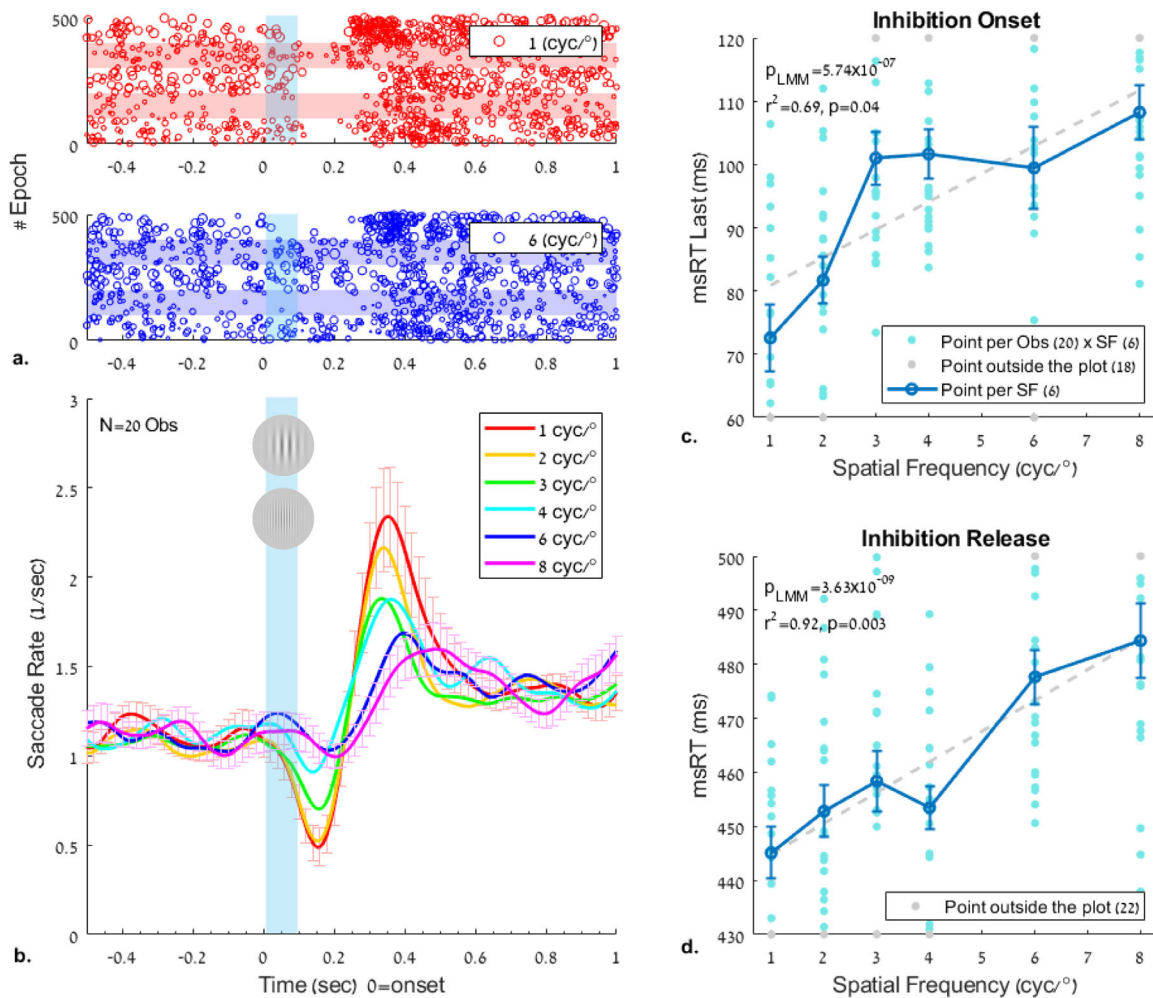


Figure 2. The effect of the spatial frequency of a flashed Gabor on the modulation of the microsaccade rate and the reaction time (msRT) during pursuit. The Gabor patches had a fixed contrast of 50% and a varied spatial frequency of 1, 2, 3, 4, 6, and 8 cyc/° (see Figure 1). (a) Example raster plots of microsaccade onsets of five observers, 100 epochs per observer (denoted by light horizontal bars), 500 epochs in total for 1 and 8 cyc/°; each row represents one epoch and each dot one microsaccade, with the dot size proportional to the microsaccade size. (b) Rate-modulation functions of microsaccades for different spatial frequencies, time-locked to the stimulus onset (time 0). (c, d) The msRT. The average across observers is shown in dark blue. The light blue dots represent each observer's average msRT in each spatial frequency, with data points outside the plot area denoted in gray at the plot border. (c) Inhibition onset, measured as the average onset of the last microsaccade in the early window of 0 to 200 ms; (d) Inhibition release, measured as the average onset of the first microsaccade in the time window of 200 to 800 ms. Note the roughly linear relation and the gradual increase in msRT in both windows ($p < 0.0005$ in LMM). Salient stimuli (e.g., 1 cyc/°) show a shorter msRT for both inhibition onset and release, and a higher msRT with increasing spatial frequency (e.g., 8 cyc/°). Error bars in all plots denote 1 SE of the mean across observers, following data normalization (see the Methods).

onset window and $p_{mc} = 0.001$ in the inhibition release window.

Microsaccade inhibition and contrast

The results for the effect of contrast on microsaccade inhibition during pursuit are shown in Figure 3 (see Experiment 2 in the Methods). The pattern of the results was similar to that of the spatial frequency, except that higher contrast is analogous to lower spatial

frequency (higher visibility) and contrast should be expressed in Log units. Similar to the results obtained for spatial frequency, the msRT value for both the onset (Figure 3c) and release from inhibition (Figure 3d) decreased linearly as a function of Log(contrast) from 3.125% up to 50% contrast; however, it was faster for higher contrast, with the inhibition onset at ~ 77 ms for the highest contrast and the inhibition release at ~ 442 ms at 50% contrast. The LMM statistics show the following values: $\beta_1 = -15.83$ ($-21.78, -9.87$), $SE = 2.99$, $t(86) = -5.28$ (the degree of freedom is 86 instead

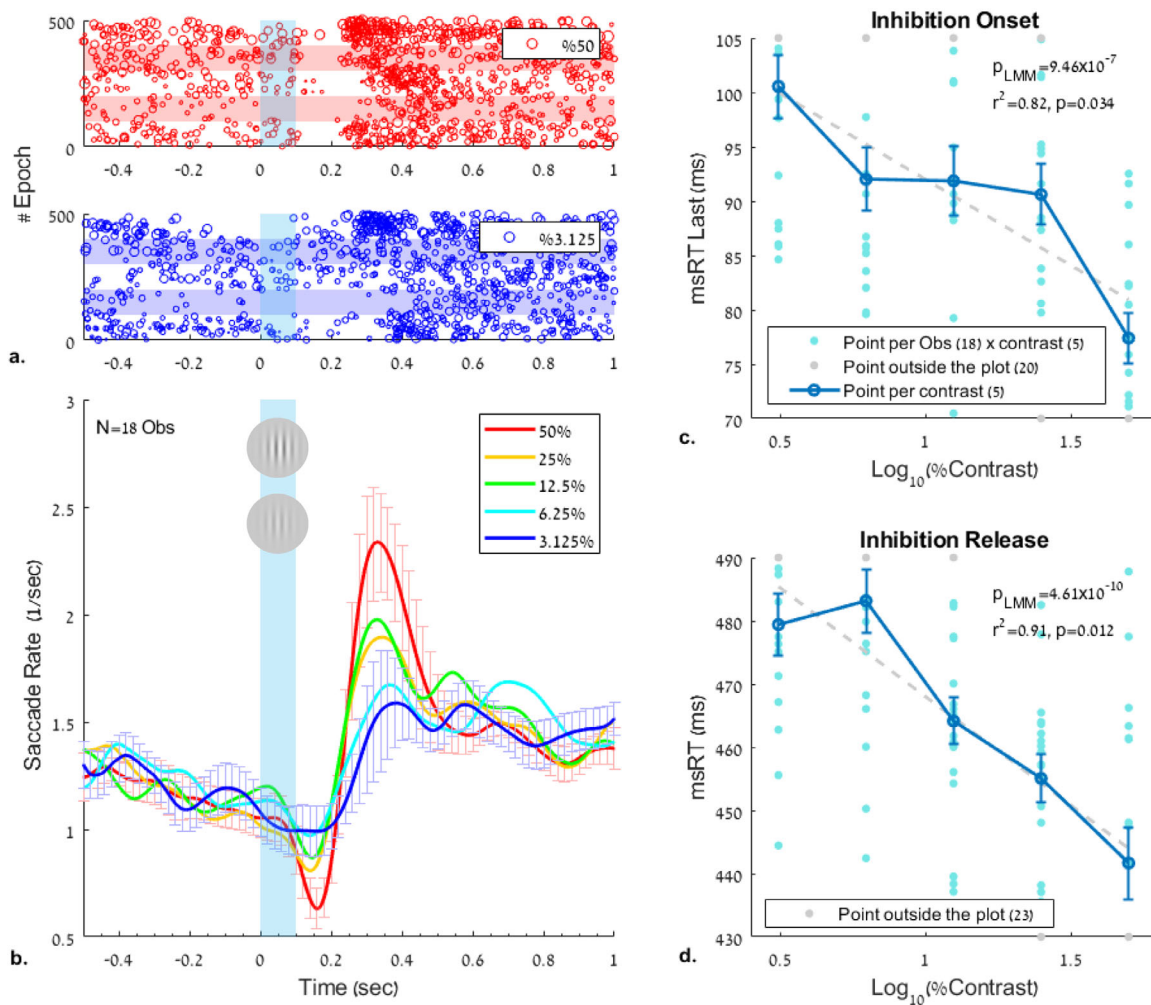


Figure 3. The effect of the contrast of a flashed Gabor on the modulation of the microsaccade rate and the reaction time (msRT) during pursuit. The Gabor patches had a fixed spatial frequency of 3 cyc/° and a varied contrast (see Figure 1). The results and analyses were similar to the effect of spatial frequency. (a) Example of the raster plots of microsaccade onsets of five observers, 100 epochs per observer (denoted by *light horizontal bars*), 500 epochs in total for 50% and 3.125% contrast (the same subjects appear in both graphs); each row represents one epoch and each dot one microsaccade with a dot size proportional to the microsaccade size. (b) Rate-modulation functions of microsaccades for different contrast levels, time-locked to the stimulus onset (time 0). (c, d) The msRT for the inhibition onset (c) and release (d). (c) Inhibition onset, measured as the average onset of the last microsaccade in an early window of 0 to 200 ms; (d) Inhibition release, measured as the average onset of the first microsaccade in the time window of 200 to 800 ms. *Error bars* denote 1 *SE* of the mean across observers under all conditions (normalized by data demeaning and correction, see the Methods). Note the roughly linear relation ($r^2 > 0.8$) and the gradual decrease in msRT as a function of contrast in both early and late windows. LMM shows significance ($p < 0.005$) in both the inhibition onset and its release.

of 88 because of two observers with missing data, each for one contrast) in the inhibition onset window and $\beta_1 = -34.4$ ($-44.15, -24.65$), $SE = 4.9$, $t(88) = -7.01$ in the inhibition release window. The slopes show a decrease of msRT as the contrast increases; all p values of LMM were significant ($p < 0.005$), indicating that a nonzero linear relationship exists between msRT and the $\text{log}_{10} \% \text{ contrast}$. The correlation for the inhibition onset (0–200 ms) was $r^2 = 0.82$ and for the inhibition release (200–800 ms) it was $r^2 = 0.91$, both significant ($p < 0.05$). The additional nonparametric

permutation test confirmed significance with $p_{\text{mc}} = 0.015$ in the inhibition onset window and $p_{\text{mc}} = 0.002$ in the inhibition release window.

Pursuit inhibition and spatial frequency

We analyzed the pursuit velocity modulation by the flashed Gabor patch as a function of the spatial frequency (see Experiment 1 in the Methods) following the saccade analysis above. We extracted the pursuit eye

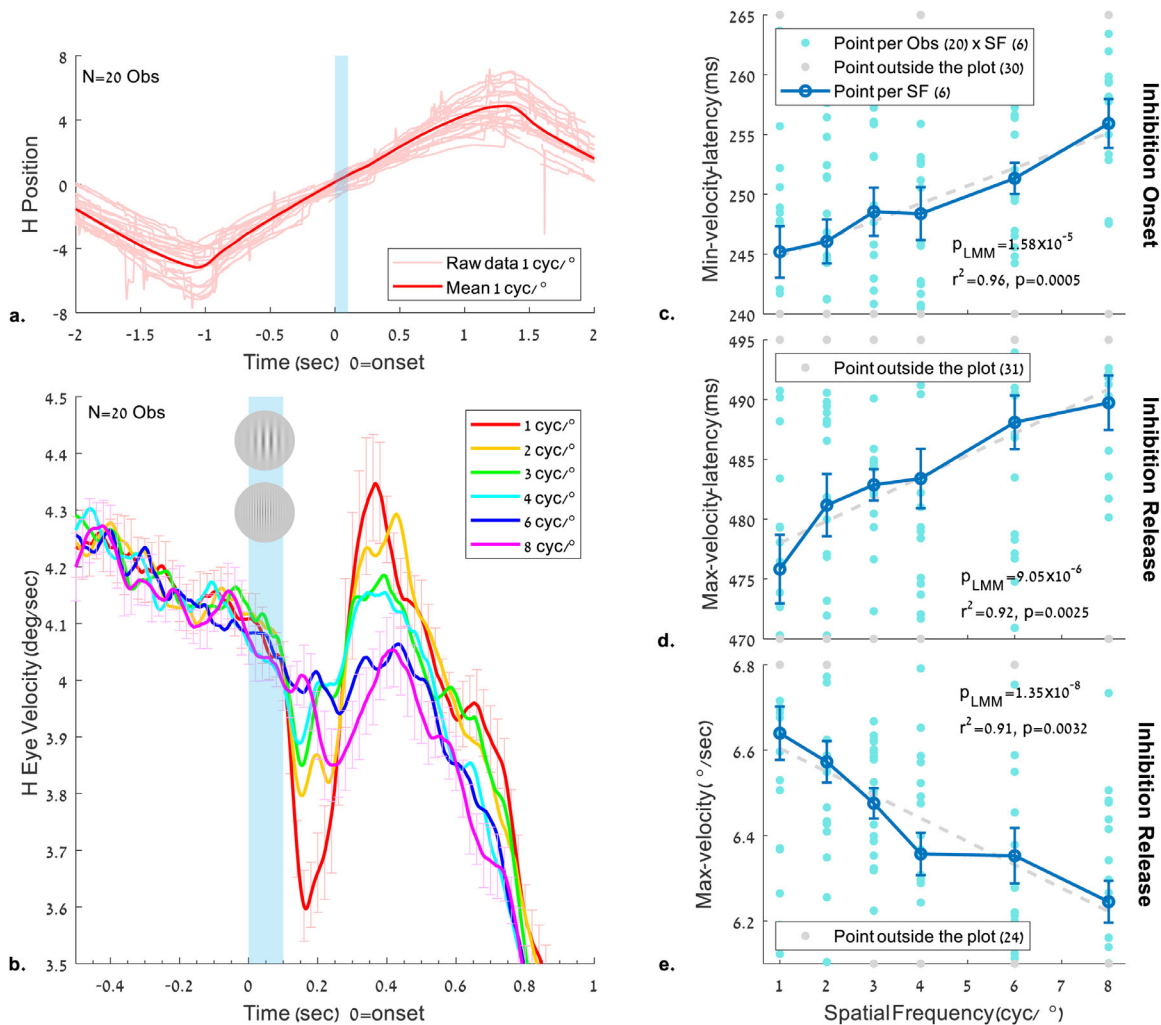


Figure 4. The effect of the spatial frequency of a flashed Gabor on the eye velocity during pursuit. The stimulus and conditions are as in Figure 2 (see also Figure 1 and the Methods). (a) Horizontal eye position of the first trial of each observer ($N = 20$) and the normalized mean across observers for the $1 \text{ cyc}/^\circ$ condition. Note the saccades during pursuit in the trial data (a faint color) and their absence around the time of the Gabor appearance. (b) Horizontal eye velocity modulation around the time of the flashed Gabor, showing “pursuit inhibition,” with velocity slowdown followed by velocity acceleration, depending on the flashed stimulus parameters. (c–e) Pursuit latency and peak velocity relative to the flashed Gabor onset as a function of its spatial frequency. (c) Latency of the minimum velocity in the time window of 100 to 400 ms; (d) Latency of the maximum velocity peak in the time window of 300 to 700 ms. (e) Maximum velocity in the time window of 300 to 700 ms. Error bars denote 1 SE of the mean across observers under all conditions (normalized by data demeaning and correction, see the Methods). As shown (plots c–e), the minima and maxima latencies in both windows increased as a function of spatial frequency, and the velocity at maxima decreased; all of the above showed a significant p value in LMM ($p < 0.005$) with a high correlation for the group average ($r^2 > 0.9$).

velocity only from the horizontal eye position, after saccade and blink removal, and explored its properties regarding latency and peak velocity (see the Methods). The results of the spatial frequency experiment appear in Figure 4. As shown in Figure 4b, the eye velocity was modulated around the time of the flashed Gabor (100 ms in blue shade); the horizontal velocity decreased to a minimum of around 200 ms and then increased to a maximum of around 400 ms. This modulation was related to the Gabor spatial frequency, with a strong modulation for low frequencies (e.g., $1 \text{ cyc}/^\circ$)

and a weak modulation for high frequencies (e.g., $8 \text{ cyc}/^\circ$). Figures 4c–4e shows the pursuit latencies and the peak velocity as a function of spatial frequency in specific time windows derived from the continuous velocity modulation function (Figure 4b): 100 to 400 ms for the inhibition and 300 to 700 ms for its release. As shown (Figures 4c–4e), the latency of the minimum and maximum velocity peaks increased, and the maximum velocity decreased with increased spatial frequency. The related effect on the minimum velocity was insignificant (data not shown). The LMM analysis revealed the same

effect, with $\beta_1 = 1.47$ (0.83,2.12), $SE = 0.33$, and $t(118) = 4.50$ at the minimum velocity latency window (4c), $\beta_1 = 1.84$ (1.05,2.62), $SE = 0.39$, and $t(118) = 4.64$ in the maximum velocity latency window (4d), and $\beta_1 = -0.05$ (-0.07, -0.04), $SE = 0.009$, and $t(118) = -6.10$ in the peak velocity window (4e); all p values of the LMM model were significant ($p < 0.005$), indicating that a nonzero linear relationship exists between the pursuit latencies and the maximum pursuit velocity for the spatial frequencies tested. The correlation of the mean results were all linear for the group averages: for the minimum velocity latency ($r^2 = 0.96$), the maximum velocity latency ($r^2 = 0.92$), and the peak velocity ($r^2 = 0.91$), the p -values of the correlations were all found to be significant ($p < 0.005$). The nonparametric permutation test revealed additional significant results, with $p_{mc} = 0.001$ in the minimum velocity latency, $p_{mc} = 0.001$ in the maximum velocity latency, and $p_{mc} = 0.002$ in the peak velocity.

Pursuit inhibition and contrast

The results for the velocity modulation time course and the latencies in the contrast experiment are shown in Figure 5 (see Experiment 2 in the Methods); they are similar to the results obtained for spatial frequency (Figure 4), except that higher contrast is analogous to lower frequency. Figure 5 shows that after a Gabor patch with 50% contrast is flashed, there is an initial slowdown and then a fast increase in speed. These velocity perturbations decreased with lower contrast. Figures 5c to 5e show the pursuit latencies and the peak velocity as a function of the \log_{10} contrast percentage in the same time windows used for analyzing the spatial frequency: 100 to 400 ms for the inhibition and 300 to 700 ms for its release. The LMM shows values of $\beta_1 = -6.68$ (-10.8, -2.56), $SE = 2.07$, and $t(88) = -3.22$ in the minimum velocity latency window (5c), $\beta_1 = -13.06$ (-18.95, -7.18), $SE = 2.96$, and $t(88) = -4.41$ in the maximum velocity latency window (5d), and $\beta_1 = 0.25$ (0.09,0.41), $SE = 0.08$, and $t(88) = 3.09$ in the peak velocity window. As shown, the latency of the minimum and maximum velocity peaks decreased (negative slopes) when the contrast increased, and the maximum velocity increased (positive slope) along with increased contrast. The related effect on the minimum velocity was insignificant (data not shown). All LMM p values were significant ($p < 0.005$), indicating that a nonzero linear relationship exists between the pursuit latencies and the maximum pursuit velocity for the log contrast tested. The linear correlations for the group averages are as follows: for the minimum velocity latency ($r^2 = 0.81$), the maximum velocity latency ($r^2 = 0.85$), and the peak velocity ($r^2 = 0.69$), with significance ($p < 0.05$) found for the minimum and maximum latencies, but not for the peak velocity. The

nonparametric permutation test revealed significant results with $p_{mc} = 0.025$ in the minimum velocity latency, $p_{mc} = 0.013$ in the maximum velocity latency, and $p_{mc} = 0.043$ in the peak velocity.

The relationship between pursuit inhibition and catch-up saccade inhibition

To investigate the relationship between pursuit inhibition and catch-up saccade inhibition during smooth pursuit, we present a correlation matrix for the spatial frequency trials (Experiment 1) in Figure 6, and one for the contrast trials (Experiment 2) in Figure 7. These correlation matrices show the links between all OMI measures presented in Figures 2 to 5 in the same time window fixed for each measurement. The group averages are presented above the diagonal, and the individual observer results (one dot per observer) are presented under the diagonal. The different correlation values and their significant p values were noted on each correlation plot, with significant values denoted in red. Note that most of the OMI correlations in the spatial frequency trials (Figure 6) were significant except the group average of the msRTs' inhibition onset and inhibition release, in addition to the individual correlations between msRT in the inhibition onset window and the maximum and minimum velocity latency. Note the significant correlations in the inhibition release time windows of msRT (200-800 ms) and the maximum velocity latency (300-700 ms) in both the spatial frequency trials (Figure 6) and the contrast trials (Figure 7).

Smooth pursuit without distractors

In an additional control experiment, we measured smooth pursuit without a flashed Gabor presentation in an otherwise identical paradigm as in the other experiments (see Experiment 3 in the Methods). The results showed a steady velocity (data not shown) around the time of Gabor flashing in the other experiments, suggesting that any perturbation in pursuit velocity is driven by the external stimuli. Additionally, no significant velocity difference existed between the left and right tracking; therefore both traces were pooled together.

Pursuit inhibition and contrast sensitivity

We investigated the relationship between microsaccade and pursuit inhibition during smooth pursuit and contrast sensitivity, as was previously done for the static fixation (Bonneh et al., 2015). For

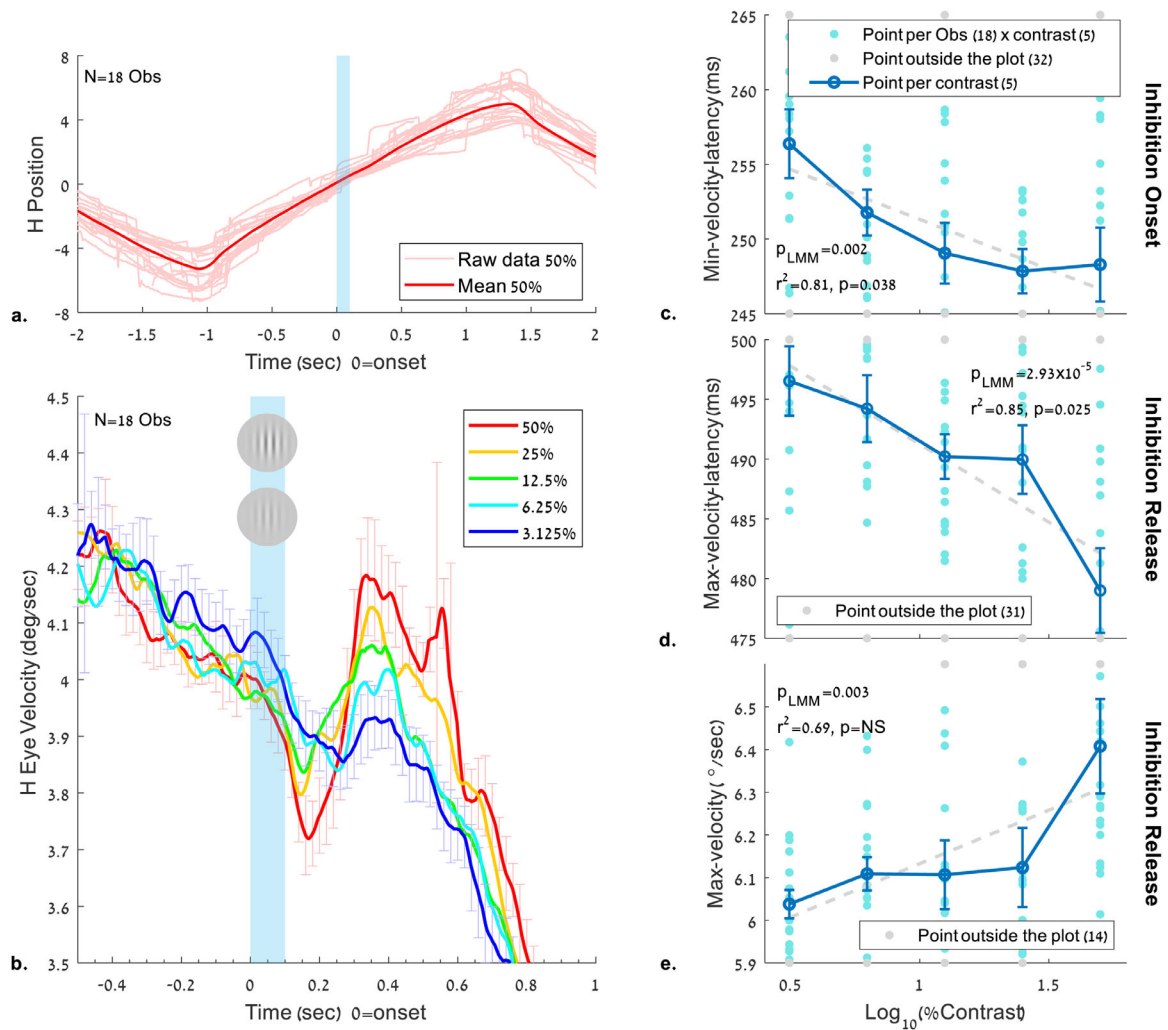


Figure 5. The effect of the contrast of a flashed Gabor on the eye velocity during pursuit. The stimulus and conditions are the same as in Figure 3, and the analyses are the same as in Figure 4 (see also Figure 1 and the Methods). (a) Horizontal eye position of the first trial of each observer ($N = 18$) and the normalized mean across observers for the 50% contrast condition. (b) Horizontal eye velocity modulation around the time of the flashed Gabor, showing “pursuit inhibition” (slowdown then acceleration), depending on the flashed stimulus contrast. (c–e) Pursuit latency and peak velocity relative to the flashed Gabor onset as a function of its contrast, quantified in the same time windows as in Figure 4. (c) Latency to the minimum velocity in the time window of 100 to 400 ms; (d) Latency to the maximum velocity peak in the time window of 300 to 700 ms. (e) Maximum velocity showing inhibition release in the time window of 300 to 700 ms. Error bars denote 1 SE of the mean across observers under all conditions (normalized by data demeaning and correction; see the Methods). As shown (plots c–e), the minima and maxima latencies in both windows decreased as a function of contrast (shorter latencies at high contrast), and the velocity at maxima increased with contrast. Note the significant correlation of latencies with contrast (c, d) for the group average ($r^2 > 0.8$). LMM shows a significant p value ($p < 0.005$) with all OMI measures (c–e).

this purpose, we conducted separate psychophysical experiments to examine the contrast detection thresholds at the same spatial frequencies tested in experiment 1 with 12 observers (see Experiment 4 in the Methods). The results are shown in Figures 8 and 9. All OMI and threshold results were converted to Z-values (subtracting the mean and dividing by the SD per observer). Figure 8 shows a similar trend for all OMI measures introduced in Figures 2–5 and the contrast

detection threshold. To highlight the similarity of the OMI trends to the threshold, the maximum velocity data in a time window of 300 to 700 ms were multiplied by -1 to reverse the slope. Figure 9 show the correlation matrix of all OMI measures with the contrast detection thresholds; the plots above the diagonal represent correlations for the group average for each spatial frequency and the plots under the diagonal represent the correlations computed for individual observers

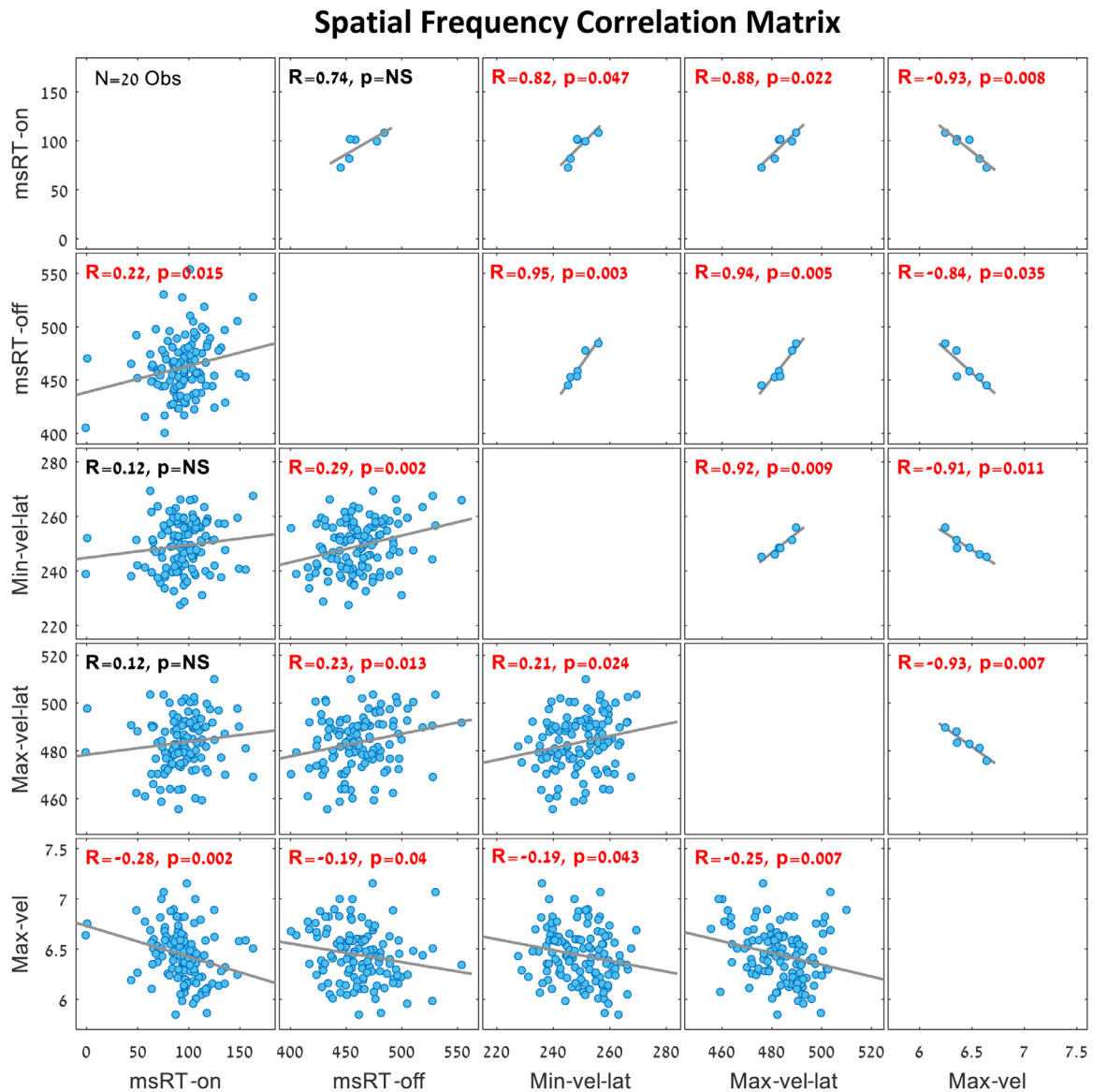


Figure 6. Correlation matrix of OMI measures during smooth pursuit in the spatial frequency trials ($N = 20$ observers with six spatial frequencies). The plots above the diagonal show the group averages for each spatial frequency (six dots, one per each spatial frequency), and the plots under the diagonal show correlations across individual observers (one dot per observer and spatial frequency). Significant correlations ($p < 0.05$) are denoted in red. Note the significant linear correlations in the inhibition release window between msRT (200–800 ms) and the maximum velocity latency (300–700 ms), with $R = 0.94$ in the group average and $R = 0.23$ in the individual observers' data. This represents an increase in latency, along with a decrease in stimulus visibility in both OMI measures. When correcting for multiple comparisons (10), some correlations become insignificant, but the combined picture is clear.

(one point per observer and frequency). Note the significant correlations of the Minimum velocity latency (100–400 ms), msRT at the inhibition release (200–800 ms), and the maximum peak velocity (300–700 ms), in both the individual data and the averaged data across conditions. The correlations between the detection threshold and the OMI measures were as follows: (1) msRT for the inhibition onset (0–200 ms), individuals: $R = 0.42, p = 0.0003$, and group averages: $R = 0.69$,

$p = NS$ (0.12); (2) msRT for the inhibition release (200–800 ms), individuals: $R = 0.65, p = 5.8 \times 10^{-10}$, group averages: $R = 0.96, p = 0.002$; (3) minimum velocity latency, individuals: $R = 0.36, p = 0.002$, group averages: $R = 0.88, p = 0.02$; (4) maximum velocity latency, individuals: $R = 0.22, p = NS$ (0.06), group averages: $R = 0.80, p = NS$ (0.057); (5) maximum velocity, individuals: $R = (-0.32), p = 0.006$, group averages: $R = (-0.86), p = 0.03$.

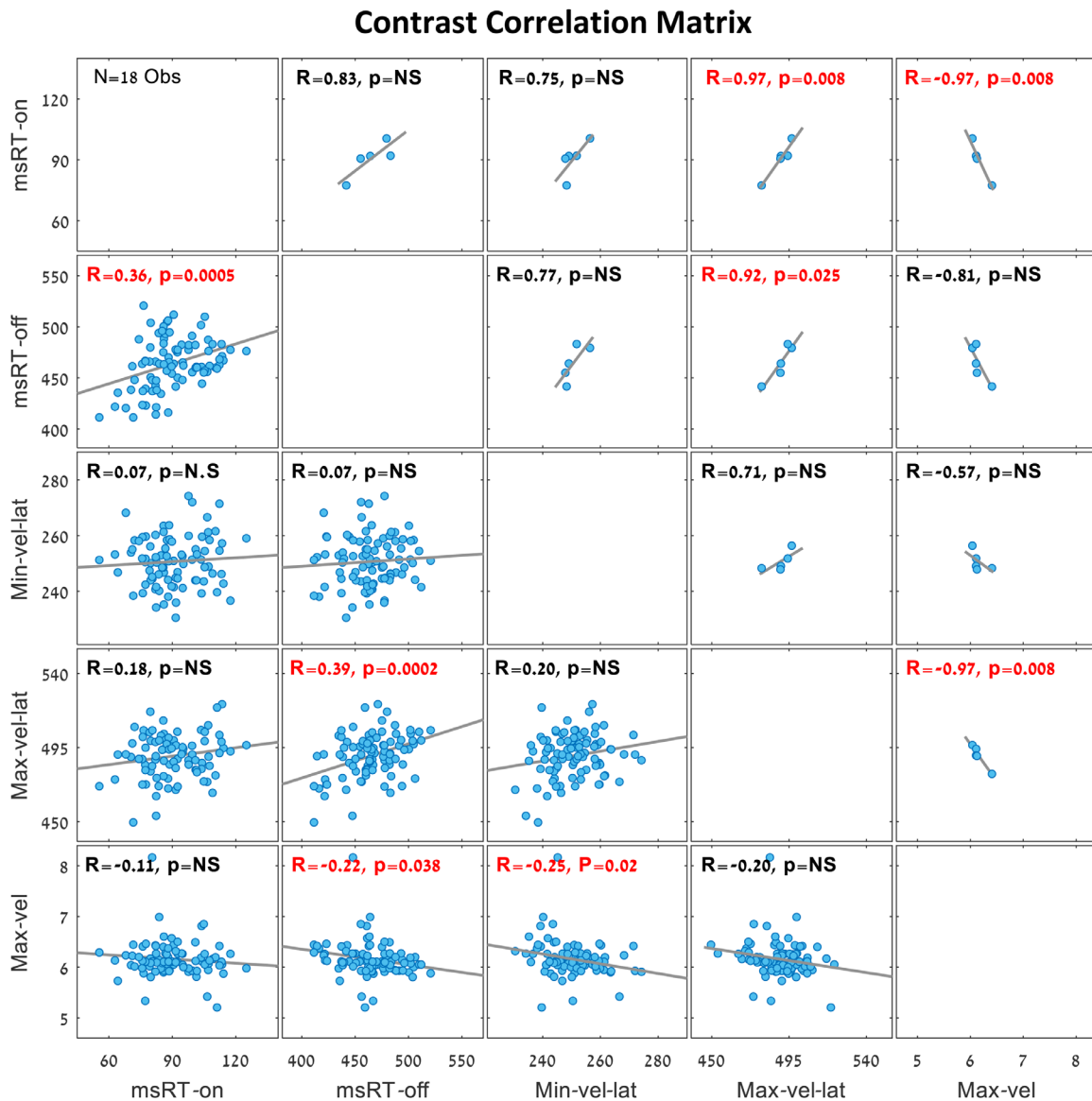


Figure 7. Correlation matrix of OMI measures during smooth pursuit in the contrast trials ($N = 18$ observers with five contrast levels). The plots above the diagonal show the group average for each contrast (five dots, one for each contrast) and the plots below the diagonal show the correlations of individual observers (one dot per observer and contrast). Significant correlation values are denoted in red. Note the significant linear correlations in the inhibition release window between msRT (200–800 ms) and the maximum velocity latency (300–700 ms), with $R = 0.92$ for the group average and $R = 0.39$ for the individual observers' data. This represents an increase in latency, along with a decrease in stimulus visibility in both OMI measures. When correcting for multiple comparisons (10), some correlations become insignificant, but the combined picture is clear.

Microsaccade RT during fixation versus smooth pursuit

A comparison between microsaccade RTs during fixation and smooth pursuit is shown in Figure 10. The results of msRT at fixation as a function of contrast (Figures 10a, 10b) were taken from Bonneh et al. (2015), whereas the results of the msRT at fixation as a function of spatial frequency (Figures 10c, 10d) were

measured in the present study (see Experiment 5 in the Methods). The msRT trends during fixation and pursuit were plotted in the relevant time windows for each experiment, that is, contrast and spatial frequency. The results show a ~ 20 ms delay for the inhibition onset of saccades during pursuit compared with fixation (Figures 10a, 10c). The inhibition onset represents the latency of the last microsaccade in an early time window (see the caption for more details). Note that a

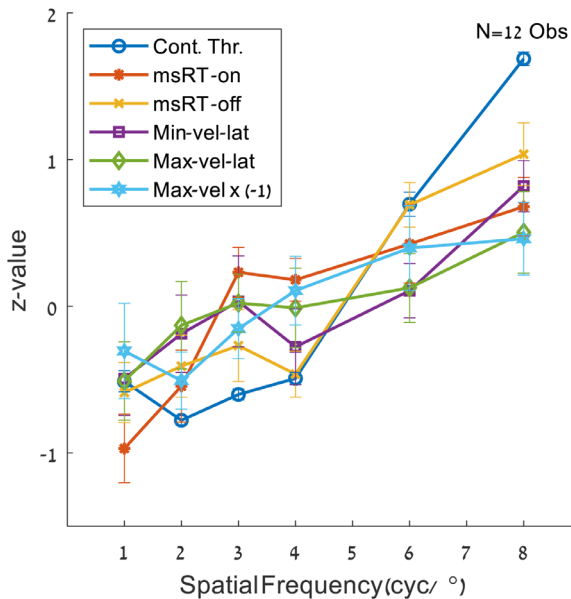


Figure 8. Contrast detection thresholds and oculomotor measures. The data were obtained from the spatial frequency and contrast sensitivity (psychophysics) experiments, for the spatial frequencies of 1, 2, 3, 4, 6, and 8 cyc/°; they were converted to Z-values per observers by subtracting the mean and dividing by the standard deviation. Note the similar trend for all displayed parameters. The maximum velocity values are multiplied by -1 to point out the trend.

few differences exist in the stimuli and the time windows between the current experiment and that of [Bonneh et al. \(2015\)](#), which we used for comparing the contrast conditions: $\sigma = 2.7^\circ$ for the Gabor envelopes in the static fixation study, compared with $\sigma = 1.24^\circ$ in the current pursuit study, and a slight difference in the time windows for the msRT calculation. Despite these differences, the slopes of msRT as a function of contrast were very similar. There was also a slight difference between the two trends in [Figure 10d](#) (see 1cyc/°); this difference can reflect a change in the experimental conditions in Experiment 5 (a no-Gabor condition was randomized with the remaining spatial frequencies).

Discussion

In our study we briefly flashed a Gabor patch during steady-state smooth pursuit. We found a catch-up saccade inhibition in saccades with the size of microsaccades ($<2^\circ$) as well as a pursuit speed inhibition. The inhibition pattern in both cases was stimulus dependent, with a stronger and shorter inhibition for more salient stimuli, that is, a higher contrast and lower spatial frequency, suggesting a generalized OMI effect. We quantified this inhibition

with a set of event-related measures that included the onset and release latency of microsaccade inhibition, as well as the magnitude and latency of the minima and maxima of pursuit speed modulation induced by the stimulus onset. Some of these inhibition measures were significantly correlated with the contrast sensitivity obtained via psychophysical measures of contrast detection thresholds in the same subjects.

Microsaccades versus catch-up saccades during smooth pursuit

All saccades included in our analyses were microsaccades according to their size ($<2^\circ$). To investigate the type of microsaccade involved in OMI during smooth pursuit, we analyzed the direction of the microsaccades in the relevant time window of inhibition onset (0-200 ms) and release (200-800 ms), as used in the msRT analyses ([Figures 2 and 3](#)), shown in Supplementary Figures S1 and S2. When the catch-up saccade direction was inspected, more than 80% of the saccades in the spatial frequency trials (Supplementary Figure S1) and more than 76% of the saccades in the contrast trials (Supplementary Figure S2) were in the direction of motion (forward saccades). This pattern of results persisted for microsaccades smaller than 0.5° , with more than 75% forward saccades in the spatial frequency trials and more than 68.3% forward saccades in the contrast trials. When inspecting the microsaccade rate modulation of backward saccades, that is, opposite the pursuit direction (Supplementary Figure S3), we obtained an inhibition pattern like that obtained with all saccades (compare it to [Figures 2 and 3](#)). Moreover, the msRT of the backward saccades (not shown) showed significant effects (p values in LMM) in all windows except for the spatial frequency in the inhibition release window; however, this could be due to the low number of backward saccades. Recently it was shown that small saccades of a similar size could be classified according to their function, e.g., goal-directed or not ([Sinn & Engbert, 2016](#)). In our case, the small catch-up saccades had a clear function and destination, whereas microsaccades during fixation did not. However, all of the microsaccades, regardless of their direction (during pursuit) or function (catch-up or fixational), provided a very similar involuntary measure of low-level visual properties ([Bonneh et al., 2015; Bonneh et al., 2016](#)).

Fixational microsaccades versus catch-up saccades

In our study microsaccade RTs in fixation and in smooth pursuit exhibited a similar pattern ([Figure 10](#)).

Contrast Thresholds and the OMI Correlation Matrix

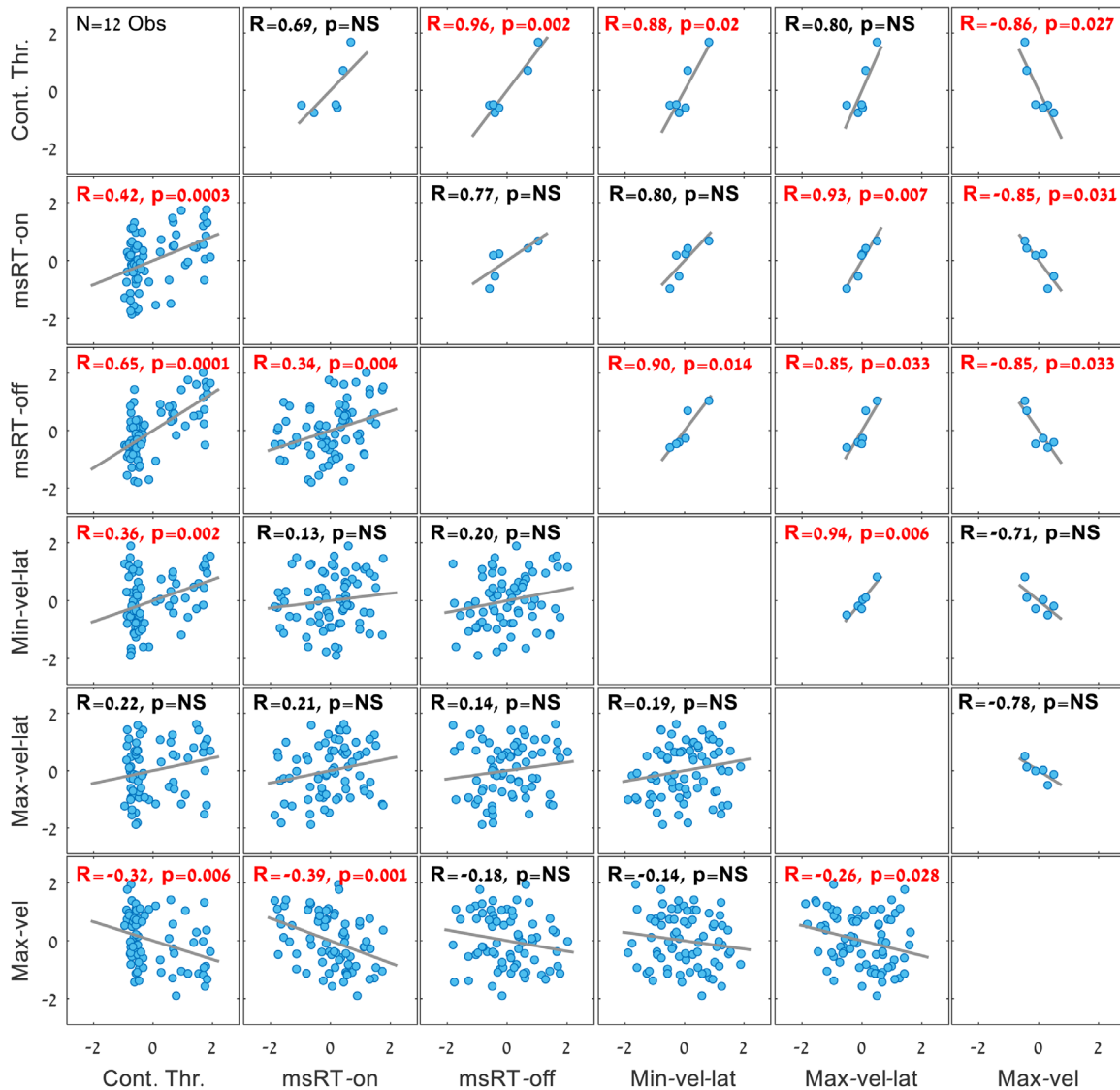


Figure 9. Correlation matrix of the contrast detection thresholds and the oculomotor measures. The data were obtained from the spatial frequency and contrast sensitivity (psychophysics) experiments, as in Figure 8. The data were converted to Z-values per observer by subtracting the mean and dividing by the standard deviation. The plots above the diagonal show the group average for each spatial frequency (six dots, one for each spatial frequency) and the plots under the diagonal show correlations of individual observers (one dot per observer and spatial frequency). Significant correlation values are denoted in red. Note the significant correlations between the threshold and the minimum velocity latency (at 100–400 ms) as in Figure 4c, the correlation between the threshold and msRT from the inhibition release window (200–800 ms) as in Figure 1d, and the correlation between the threshold and the peak velocity as in Figure 4e. When correcting for multiple comparisons (15), some correlations become insignificant, but the combined picture is clear.

However, there is an interesting global difference of about ~ 20 ms delay in the inhibition onset for pursuit (Figures 10a, 10c), in contrast to no such difference for the inhibition release latency (Figures 10b, 10d). This apparent ~ 20 ms slowdown in the onset of inhibition could indicate a longer latency of the flash signal transfer during pursuit. Alternatively, the delay could

be derived from the triggering process of catch-up saccades, which according to our current models, involves an additional processing of prediction, velocity, and position errors (de Brouwer, Yuksel, et al., 2002; Nachmani et al., 2020). In general, our results indicate that microsaccade inhibition can be measured either when the observer fixates on a static fixation point or

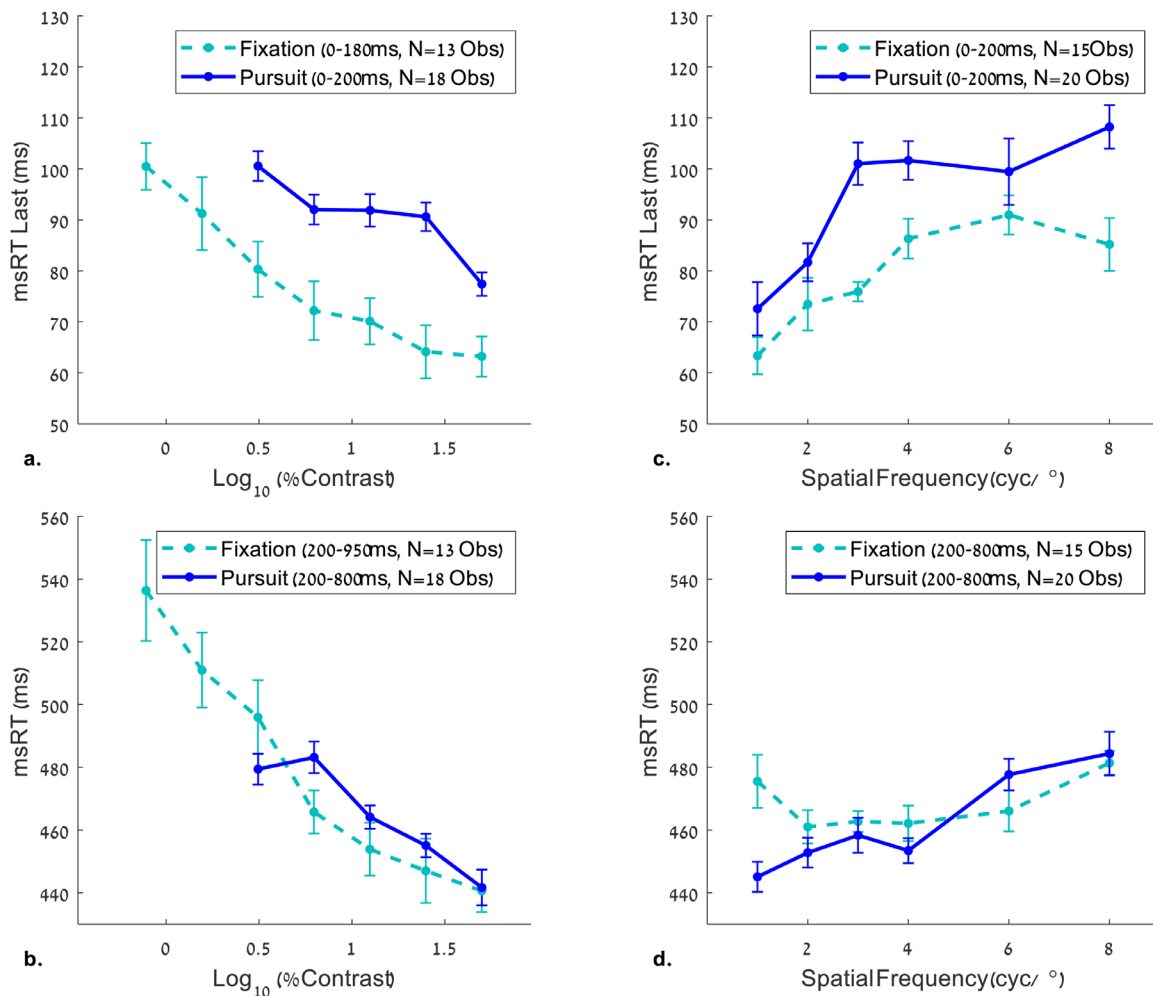


Figure 10. Comparison between OMI measures for static fixation and smooth pursuit. The msRT values were plotted in the early (a, c) and late (b, d) windows for contrast (a, b) and spatial frequency (c, d) measurements. The data for the effect of contrast during fixation (a, b) were obtained from [Bonneh et al. \(2015\)](#). Note the longer microsaccade RT for the pursuit, compared to static fixation in the inhibition onset windows (a, c), but not in the inhibition release windows (b, d). The reliability of this comparison is limited by a few small differences between the current study and that of [Bonneh et al. \(2015\)](#), including Gabor size (twice as small in our study) and the time windows used for msRT extraction (a small difference; see the legend).

tracks a moving target; it provides similar involuntary measures for the observer's response to contrast and spatial frequency.

Pursuit inhibition as a possible side effect of microsaccade inhibition

We investigated whether pursuit inhibition could be a side effect of microsaccade inhibition, or alternatively, a separate phenomenon. Although saccades were removed from the horizontal trace with margins, to prevent their effect on pursuit velocity, they still could have affected the horizontal trace. Previous studies of fixational eye movements found

a decrease in ocular drift before microsaccade onset ([Engbert & Mergenthaler, 2006](#)), whereas others found enhancement after microsaccade onset ([Chen & Hafed, 2013](#)). When applied to pursuit, this could explain pursuit inhibition as a byproduct of saccadic inhibition. To explore this possibility, we examined eye velocity in epochs that did not include any saccade in the time range of 500 ms pre to 800 ms post-stimulus onset in experiments 1 and 2 (see the Methods). There were relatively few of these epochs (~186 epochs across all observers at 1 cyc/° and ~117 epochs at 50% contrast). The results appear in Supplementary Figure S4, showing that the modulation of the horizontal eye velocity was present even in epochs without saccades. This suggests that pursuit inhibition is not a side effect of microsaccade inhibition.

Pursuit inhibition as a result of vector averaging

When two stimuli with different velocities and directions are presented simultaneously at pursuit initiation, the initial pursuit often follows the weighted vector average of the stimuli, until target selection or the occurrence of a saccade (Kleinschmidt, Büchel, Hutton, Friston, & Frackowiak, 2002; Lisberger & Ferrera, 1997). However, this rule does not apply when there are cues for target selection or there are instructions to ignore one of the targets (Blohm, Missal, & Lefèvre, 2005; Garbutt & Lisberger, 2006; Kerzel, Souto, & Ziegler, 2008; Spering, Gegenfurtner, & Kerzel, 2006). In our experiments, the flashed stimulus that caused the inhibition was presented at the center of the gaze; therefore it is unlikely to be ignored. It could have added zero velocity to a vector averaging mechanism and therefore impede the pursuit velocity with weights that represent the contrast and spatial frequency of the flashed stimulus inducing the “pursuit inhibition.” The alternative explanation that we propose here attributes pursuit inhibition to a general OMI mechanism. This general explanation implies that higher-level effects such as face familiarity (Rosenzweig & Bonneh, 2019) or cross-modal effects should be found for pursuit inhibition as well. Indeed, Kerzel et al. (2010) found pursuit inhibition in response to sound, although the effect was small. This line of investigation remains for future work.

Comparing pursuit modulation by transient stimuli to previous studies

Several studies examined the effect of transient stimuli on smooth pursuit, but unlike in our study, these stimuli were far from fixation (Buonocore et al., 2019; Kerzel et al., 2010). Buonocore et al. (2019) examined the effect of forward, backward, or a full flash on pursuit velocity and found that the pursuit velocity was altered according to the flashed location and that catch-up saccades were inhibited similarly to microsaccades in fixation. Our results are consistent with the findings for the full-flash condition in sustained smooth pursuit, whereas the other conditions are incomparable. Kerzel et al. (2010) found catch-up saccade inhibition and pursuit inhibition in steady-state smooth pursuit induced by two peripheral (5°) flashed Gabor stripes with varied contrast (4%-100%). By contrast, we found a consistently earlier onset and a shorter duration of pursuit inhibition and catch-up saccade inhibition for higher contrast (Figures 3c and 5c for earlier, Figures 3d and 5d for shorter inhibition). However, Kerzel et al. (2010) found the opposite—a longer pursuit and catch-up saccade inhibition for the 100% contrast condition, which could be due to some

differences in their methods. We noted that our results are not based on specific data points, but instead on the lawful behavior and the general trends of OMI as a function of contrast.

Pursuit inhibition and contrast sensitivity

Several studies compared contrast sensitivity during fixation and smooth pursuit (Flipse et al., 1988; Murphy, 1978; Schütz, Braun, et al., 2007; Schütz, Braun, Kerzel, & Gegenfurtner, 2008; Schütz, Delipetkos, et al., 2007); identical detection thresholds were found when the stimulus was presented in the middle of the display (Flipse et al., 1988; Murphy, 1978), allowing us to compare pursuit and static fixation measures. Although in our eye tracking experiments we do not measure contrast sensitivity directly, our oculomotor measures, obtained in passive viewing, were correlated relatively well with the detection thresholds measured separately with the same participants (Figures 8 and 9). This includes all of our OMI measures except for the maximum velocity latency. This implies that the relative contrast sensitivity can be measured via the effect of OMI during smooth pursuit for stimuli presented at fixation.

Is there a common OMI mechanism?

Pursuit inhibition implies that transient stimuli or perceptual events that occur during smooth pursuit impede the pursuit speed itself, with a magnitude that is proportional to the saliency of the transient stimulus, possibly reflecting the processing time required. In analogy, this would be similar to slowing down one's walking or driving speed when a cognitive or perceptual event occurs. The same principle has previously been shown for microsaccades during fixation. We showed the same principle for microsaccades during steady-state smooth pursuit, namely, catch-up saccades (<2°). Similar to our findings, previous studies showed similarities between catch-up saccade inhibition and microsaccade inhibition (Badler et al., 2019; Buonocore et al., 2019; Kerzel et al., 2010), as well as pursuit inhibition (Buonocore et al., 2019; Kerzel et al., 2010) in response to transient visual stimuli. Our results strengthen these findings by showing a systematic correlation between OMI (microsaccades and pursuit) induced by flashed stimuli in the middle of a steady-state pursuit trajectory and OMI at fixation. Some articles suggest a common mechanism for stopping smooth pursuit and saccades (Krauzlis, Goffart, & Haged, 2017; Missal & Keller, 2002; Missal & Heinen, 2017). Our results support this hypothesis and add to our previous findings on microsaccade and blink inhibition (Bonneh, Adini & Polat, 2015; Bonneh,

Adini & Polat, 2016; see also Bonneh et al., 2014 on drift), suggesting a general mechanism that inhibits motor activity while processing previous stimuli.

Keywords: microsaccade inhibition, pursuit inhibition, contrast sensitivity, eye movements

Acknowledgments

Commercial relationships: none.

Corresponding author: Yoram Bonneh.

Email: yoram.bonneh@gmail.com.

Address: Bar-Ilan University, 5290002, Ramat-Gan, 5290002, Israel.

References

- Badler, J. B., Watamaniuk, S. N. J., & Heinen, S. J. (2019). A common mechanism modulates saccade timing during pursuit and fixation. *Journal of Neurophysiology*, *122*, 1981–1988, <https://doi.org/10.1152/jn.00198.2019>.
- Bahill, A. T., Clark, M. R., & Stark, L. (1975). The main sequence, a tool for studying human eye movements. *Mathematical Biosciences*, *24*(3–4), 191–204, [https://doi.org/10.1016/0025-5564\(75\)90075-9](https://doi.org/10.1016/0025-5564(75)90075-9).
- Barlow, H. B. (1952). Eye movements during fixation. *The Journal of Physiology*, *116*, 290–306, <https://doi.org/10.1113/jphysiol.1952.sp004706>.
- Blohm, G., Missal, M., & Lefèvre, P. (2005). Direct Evidence for a Position Input to the Smooth Pursuit System. *Journal of Neurophysiology*, *94*, 712–721, <https://doi.org/10.1152/jn.00093.2005>.
- Bonneh, Y., Adini, Y., Sagi, D., Tsodyks, M., Fried, M., & Arieli, A. (2013). Microsaccade latency uncovers stimulus predictability: Faster and longer inhibition for unpredicted stimuli. *Journal of Vision*, *13*, 1342–1342, <https://doi.org/10.1167/13.9.1342>.
- Bonneh, Y., Fried, M., Arieli, A., & Polat, U. (2014). Microsaccades and drift are similarly modulated by stimulus contrast and anticipation. *Journal of Vision*, *14*, 767–767, <https://doi.org/10.1167/14.10.767>.
- Bonneh, Y. S., Adini, Y., & Polat, U. (2015). Contrast sensitivity revealed by microsaccades. *Journal of Vision*, *15*, 11, <https://doi.org/10.1167/15.9.11>.
- Bonneh, Y. S., Adini, Y., & Polat, U. (2016). Contrast sensitivity revealed by spontaneous eyeblinks: Evidence for a common mechanism of oculomotor inhibition. *Journal of Vision*, *16*(7), 1, <https://doi.org/10.1167/16.7.1>.
- Bonneh, Y. S., Donner, T. H., Sagi, D., Fried, M., Cooperman, A., Heeger, D. J., . . . Arieli, A. (2010). Motion-induced blindness and microsaccades: Cause and effect. *Journal of Vision*, *10*(14), 22–22, <https://doi.org/10.1167/10.14.22>.
- Buonocore, A., Skinner, J., & Hafed, Z. M. (2019). Eye position error influence over “open-loop” smooth pursuit initiation. *The Journal of Neuroscience*, *39*, 2709–2721, <https://doi.org/10.1523/JNEUROSCI.2178-18.2019>.
- Chen, C.-Y., & Hafed, Z. M. (2013). Postmicrosaccadic enhancement of slow eye movements. *Journal of Neuroscience*, *33*, 5375–5386, <https://doi.org/10.1523/JNEUROSCI.3703-12.2013>.
- Cousineau, D. (2005). Confidence intervals in within-subject designs: A simpler solution to Loftus and Masson’s method. *Tutorials in Quantitative Methods for Psychology*, *1*, 42–45, <https://doi.org/10.20982/tqmp.01.1.p042>.
- de Brouwer, S., Missal, M., Barnes, G., & Lefèvre, P. (2002). Quantitative analysis of catch-up saccades during sustained pursuit. *Journal of Neurophysiology*, *87*, 1772–1780, <https://doi.org/10.1152/jn.00621.2001>.
- de Brouwer, S., Yuksel, D., Blohm, G., Missal, M., & Lefèvre, P. (2002). What triggers catch-up saccades during visual tracking? *Journal of Neurophysiology*, *87*, 1646–1650, <https://doi.org/10.1152/jn.00432.2001>.
- Denniss, J., Scholes, C., McGraw, P. V., Nam, S., & Roach, N. W. (2018). Estimation of contrast sensitivity from fixational eye movements. *Investigative Ophthalmology & Visual Science*, *59*, 5408, <https://doi.org/10.1167/iovs.18-24674>.
- Efron, B., & Tibshirani, R. J. (1994). *An Introduction to the Bootstrap*. Boca Raton, FL: CRC Press. Retrieved from http://cds.cern.ch/record/526679/files/0412042312_TOC.pdf.
- Engbert, R. (2006). Chapter 9 Microsaccades: a microcosm for research on oculomotor control, attention, and visual perception. *Progress in Brain Research*, *154*(SUPPL. A), 177–192, [https://doi.org/10.1016/S0079-6123\(06\)54009-9](https://doi.org/10.1016/S0079-6123(06)54009-9).
- Engbert, R., & Kliegl, R. (2003). Microsaccades uncover the orientation of covert attention. *Vision Research*, *43*, 1035–1045, [https://doi.org/10.1016/S0042-6989\(03\)00084-1](https://doi.org/10.1016/S0042-6989(03)00084-1).
- Engbert, R., & Mergenthaler, K. (2006). Microsaccades are triggered by low retinal image slip. *Proceedings of the National Academy of Sciences*, *103*, 7192–7197, <https://doi.org/10.1073/pnas.0509557103>.
- Flipse, J. P., Wildt, G. J. v. d., Rodenburg, M., Keemink, C. J., & Knol, P. G. M. (1988). Contrast sensitivity for oscillating sine wave gratings during ocular

- fixation and pursuit. *Vision Research*, 28(7), 819–826, [https://doi.org/10.1016/0042-6989\(88\)90029-6](https://doi.org/10.1016/0042-6989(88)90029-6).
- Garbutt, S., & Lisberger, S. G. (2006). Directional cuing of target choice in human smooth pursuit eye movements. *The Journal of Neuroscience: The Official Journal of the Society for Neuroscience*, 26, 12479–12486, <https://doi.org/10.1523/JNEUROSCI.4071-06.2006>.
- Ghodrati, M., Morris, A. P., & Price, N. S. C. (2015). The (un)suitability of modern liquid crystal displays (LCDs) for vision research. *Frontiers in Psychology*, 6(MAR), 1–11, <https://doi.org/10.3389/fpsyg.2015.00303>.
- Goettker, A., Braun, D. I., Schütz, A. C., & Gegenfurtner, K. R. (2018). Execution of saccadic eye movements affects speed perception. *Proceedings of the National Academy of Sciences*, 115, 2240–2245, <https://doi.org/10.1073/pnas.1704799115>.
- Heinen, S. J., Badler, J. B., & Watamaniuk, S. N. J. (2018). Choosing a foveal goal recruits the saccadic system during smooth pursuit. *Journal of Neurophysiology*, 120, 489–496, <https://doi.org/10.1152/jn.00418.2017>.
- Heinen, S. J., Potapchuk, E., & Watamaniuk, S. N. J. (2016). A foveal target increases catch-up saccade frequency during smooth pursuit. *Journal of Neurophysiology*, 115, 1220–1227, <https://doi.org/10.1152/jn.00774.2015>.
- Hohenstein, S., Matuschek, H., & Kliegl, R. (2017). Linked linear mixed models: A joint analysis of fixation locations and fixation durations in natural reading. *Psychonomic Bulletin & Review*, 24, 637–651, <https://doi.org/10.3758/s13423-016-1138-y>.
- Kerzel, D., Born, S., & Souto, D. (2010). Inhibition of steady-state smooth pursuit and catch-up saccades by abrupt visual and auditory onsets. *Journal of Neurophysiology*, 104, 2573–2585, <https://doi.org/10.1152/jn.00193.2010>.
- Kerzel, D., Souto, D., & Ziegler, N. E. (2008). Effects of attention shifts to stationary objects during steady-state smooth pursuit eye movements. *Vision Research*, 48, 958–969, <https://doi.org/10.1016/j.visres.2008.01.015>.
- Kleinschmidt, A., Büchel, C., Hutton, C., Friston, K. J., & Frackowiak, R. S. J. (2002). The neural structures expressing perceptual hysteresis in visual letter recognition. *Neuron*, 34, 659–666, [https://doi.org/10.1016/S0896-6273\(02\)00694-3](https://doi.org/10.1016/S0896-6273(02)00694-3).
- Kliegl, R. (2007). Toward a perceptual-span theory of distributed processing in reading: A reply to Rayner, Pollatsek, Drieghe, Slattery, and Reichle (2007). *Journal of Experimental Psychology: General*, 136, 530–537, <https://doi.org/10.1037/0096-3445.136.3.530>.
- Krauzlis, R. J., Goffart, L., & Hafed, Z. M. (2017). Neuronal control of fixation and fixational eye movements. *Philosophical Transactions of the Royal Society of London. Series B, Biological Sciences*, 372(1718), 20160205, <https://doi.org/10.1098/rstb.2016.0205>.
- Laubrock, J., Kliegl, R., Rolfs, M., & Engbert, R. (2010). When do microsaccades follow spatial attention? *Attention, Perception, & Psychophysics*, 72, 683–694, <https://doi.org/10.3758/APP.72.3.683>.
- Lisberger, S. G., & Ferrera, V. P. (1997). Vector averaging for smooth pursuit eye movements initiated by two moving targets in monkeys. *The Journal of Neuroscience: The Official Journal of the Society for Neuroscience*, 17, 7490–7502, Retrieved from <http://www.ncbi.nlm.nih.gov/pubmed/9295395>.
- Martinez-Conde, S., Macknik, S. L., & Hubel, D. H. (2004). The role of fixational eye movements in visual perception. *Nature Reviews. Neuroscience*, 5, 229–240, <https://doi.org/10.1038/nrn1348>.
- Missal, M., & Keller, E. L. (2002). Common inhibitory mechanism for saccades and smooth-pursuit eye movements. *Journal of Neurophysiology*, 88, 1880–1892, <https://doi.org/10.1152/jn.00060.2002>.
- Missal, M., & Heinen, S. J. (2017). Stopping smooth pursuit. *Philosophical Transactions of the Royal Society B: Biological Sciences*, 372(1718), 20160200, <https://doi.org/10.1098/rstb.2016.0200>.
- Murphy, B. J. (1978). Pattern thresholds for moving and stationary gratings during smooth eye movement. *Vision Research*, 18, 521–530, [https://doi.org/10.1016/0042-6989\(78\)90196-7](https://doi.org/10.1016/0042-6989(78)90196-7).
- Nachmani, O., Coutinho, J., Khan, A. Z., Lefèvre, P., & Blohm, G. (2020). Predicted Position error triggers catch-up saccades during sustained smooth pursuit. *ENEURO*, 7(1), ENEURO.0196–18.2019, <https://doi.org/10.1523/ENEURO.0196-18.2019>.
- Pastukhov, A., & Braun, J. (2010). Rare but precious: Microsaccades are highly informative about attentional allocation. *Vision Research*, 50, 1173–1184, <https://doi.org/10.1016/j.visres.2010.04.007>.
- Rolfs, M. (2009). Microsaccades: Small steps on a long way. *Vision Research*, 49, 2415–2441, <https://doi.org/10.1016/j.visres.2009.08.010>.
- Rolfs, M., Kliegl, R., & Engbert, R. (2008). Toward a model of microsaccade generation: The case of microsaccadic inhibition. *Journal of Vision*, 8(11), 5–5, <https://doi.org/10.1167/8.11.5>.
- Rosenzweig, G., & Bonneh, Y. S. (2019). Familiarity revealed by involuntary eye movements on the fringe of awareness. *Scientific Reports*, 9(1), 3029, <https://doi.org/10.1038/s41598-019-39889-6>.

- Scholes, C., McGraw, P. V., Nyström, M., & Roach, N. W. (2015). Fixational eye movements predict visual sensitivity. *Proceedings of the Royal Society B: Biological Sciences*, 282(1817), 20151568, <https://doi.org/10.1098/rspb.2015.1568>.
- Schütz, A. C., Braun, D. I., & Gegenfurtner, K. R. (2007). Contrast sensitivity during the initiation of smooth pursuit eye movements. *Vision Research*, 47, 2767–2777, <https://doi.org/10.1016/j.visres.2007.07.006>.
- Schütz, A. C., Braun, D. I., Kerzel, D., & Gegenfurtner, K. R. (2008). Improved visual sensitivity during smooth pursuit eye movements. *Nature Neuroscience*, 11, 1211–1216, <https://doi.org/10.1038/nn.2194>.
- Schütz, A. C., Delipetkos, E., Braun, D. I., Kerzel, D., & Gegenfurtner, K. R. (2007). Temporal contrast sensitivity during smooth pursuit eye movements. *Journal of Vision*, 7(13), 3, <https://doi.org/10.1167/7.13.3>.
- Sinn, P., & Engbert, R. (2016). Small saccades versus microsaccades: Experimental distinction and model-based unification. *Vision Research*, 118, 132–143, <https://doi.org/10.1016/j.visres.2015.05.012>.
- Spering, M., Gegenfurtner, K. R., & Kerzel, D. (2006). Distractor interference during smooth pursuit eye movements. *Journal of Experimental Psychology: Human Perception and Performance*, 32, 1136–1154, <https://doi.org/10.1037/0096-1523.32.5.1136>.
- Valsecchi, M., Betta, E., & Turatto, M. (2007). Visual oddballs induce prolonged microsaccadic inhibition. *Experimental Brain Research*, 177, 196–208, <https://doi.org/10.1007/s00221-006-0665-6>.
- White, A. L., & Rolfs, M. (2016). Oculomotor inhibition covaries with conscious detection. *Journal of Neurophysiology*, 116, 1507–1521, <https://doi.org/10.1152/jn.00268.2016>.
- Yablonski, M., Polat, U., Bonneh, Y. S., & Ben-Shachar, M. (2017). Microsaccades are sensitive to word structure: A novel approach to study language processing. *Scientific Reports*, 7(1), 3999, <https://doi.org/10.1038/s41598-017-04391-4>.
- Ziv, I., & Bonneh, Y. (2017). Microsaccades and pursuit inhibition during smooth pursuit. In *European Conference on Visual Perception*. Berlin: ECVP.
- Ziv, I., & Bonneh, Y. S. (2019). Microsaccades, Pursuit and Drift Modulations During Smooth Pursuit. *Journal of Vision*, 19(10), 302c, <https://doi.org/10.1167/19.10.302c>.